Design of the PD-FOPID Controller Based on Rain Optimization Algorithm to Improve Virtual Inertia Control Performance in Islanded Microgrids

F. Amiri*(C.A.), M.H. Moradi**

Abstract: Low inertia is one of the most important challenges for frequency maintenance in islanded microgrids. To address this issue, the innovative concept of Virtual Inertia Control (VIC) has emerged as a promising solution for enhancing frequency stability in such systems. This paper presents an advanced controller, the PD-FOPID, as a highly effective technique for improving the efficiency of VIC in islanded microgrids. By leveraging the Rain Optimization Algorithm (ROA), this approach enables precise fine-tuning of the controller's parameters. A key advantage of the proposed method is its inherent resilience to disruptions and uncertainties caused by parameter fluctuations in islanded microgrids. To evaluate its performance and compare it with alternative control methods, extensive assessments were conducted across various scenarios. The comparison includes VIC based on an H-infinity controller (Controller 1), VIC based on an MPC controller (Controller 2), Adaptive VIC (Controller 3), VIC based on an optimized PI controller (Controller 4), conventional VIC (Controller 5), and systems without VIC (Controller 6). The results demonstrate that the proposed methodology significantly outperforms existing approaches in the field of VIC. The simulations were conducted using MATLAB software.

1 Introduction

AN islanded microgrid's intrinsic inertia has a major impact on its frequency stability [1]. Power-electronic converters are commonly used to enable the interchange of power between the microgrid and energy sources like WT and PV because of their low moment of inertia [2, 3]. However, this low inertia poses a serious problem, endangering the microgrid's frequency stability [4]. Numerous control loops have been thoroughly investigated for frequency regulation in islanded microgrids in order to overcome this problem. They are as follows: 1) VIC, 2) PC, and 3) SC [5]. These

strategies seek to improve the system's overall frequency stability and lessen the effects of low inertia. Interestingly, although the other control loops in the microgrid remain slow, the VIC control loop is dynamic and sensitive to changes in load [6]. The quantity of kinetic energy stored in the spinning components of the microgrid is a major factor in its ability to adjust to changes in load [7]. During sudden fluctuations in load, this kinetic energy serves as a buffer to assist the system in maintaining frequency stability [8]. It is feasible to increase the microgrid's resistance to these disruptions and guarantee dependable functioning by utilizing sophisticated control techniques [9, 10].

The microgrid's inertia determines whether kinetic energy is absorbed or transmitted. The PC takes around 10 to 30 seconds to restore the frequency to a new stable condition after events or interruptions. In a similar manner, the SC restores the frequency to its nominal state between 30 seconds and 30 minutes following frequency aberrations. As a result, the VIC, as defined by [11], is crucial for preserving frequency stability in an

islanded microgrid. In essence, the main catalyst for enhancing and maintaining such stability is this specific element included in virtual synchronous generators [12]. Other energy storage technologies, including batteries, pumped hydro systems, and hydrogen systems, can also serve as alternate VIC components in a microgrid [12, 13]. By employing VIC technology, these energy storage devices which may be thought of as virtual sources of inertia achieve power system performance comparable to SG [14]. However, in an islanded microgrid, significant disturbances and uncertainty in parameter values pose a threat to VIC's effectiveness [15]. Several control techniques have been used to improve VIC's effectiveness against these disturbances and uncertainties brought on by system characteristics [16–42].

It was discovered in [16, 17] that using the fuzzy controller improved the VIC efficiency in islanded microgrids. However, because of its intricate and demanding design, the use of a fuzzy controller is limited. Fuzzy controllers' inefficiency in the face of internal microgrid disruptions, including load disruptions or interruptions in renewable energy sources, is a major disadvantage. The MPC controller was used in [18–20] to improve microgrid VIC efficiency. The controller can effectively provide VIC with sufficient performance by using an accurate microgrid model. It should be mentioned, nonetheless, that the MPC controller's reliance on a precise microgrid model is one of its main disadvantages. The overall performance of the system will unavoidably suffer if an accurate model is not supplied. Furthermore, MPC's effectiveness deteriorates in unclear circumstances. Researchers have looked into using an H∞ controller to improve VIC's performance in microgrids that are subject to uncertainties and interruptions [21, 22]. Specifically, this kind of controller is resilient to microgrid disturbances and works to reduce their effects as much as possible. It further exhibits robustness to uncertainty related to microgrid parameters. However, it must be recognized that one of this controller's main drawbacks is its dependence on the system model. However, the lack of an accurate model for the microgrid might decrease the H∞ controller's efficacy. Furthermore, because of its complexity, incorporating the H∞ controller into an islanded microgrid is difficult. In [23], the paper discusses a study that aims to enhance the performance of VIC within the microgrid. The improvement is achieved through the adoption of an adaptive VIC, which incorporates a bang-bang control mechanism. One of the key shortcomings of this control system is its performance degradation in the presence of disruptions and generating sources. The coefficient diagram method is used in [24] to regulate the microgrid uniquely. This

method has limitations since it requires intricate calculations and offers little protection against load variations. In addition, [25] adds a neuro-fuzzy network to the microgrid's VIC structure to regulate frequency. It is important to keep in mind, nevertheless, that applying this strategy to VIC presents computational complexity issues. To control the frequency and improve stability in the islanded microgrid, a novel method known as the RPWFNN was used inside the VIC structure [26].

When it comes to putting this strategy into practice within VIC systems, it must be acknowledged that a major obstacle is its computational complexity. Furthermore, a new and sophisticated dynamic controller has been used in [27] and [28] to enhance VIC performance in isolated microgrids with one or more regions. This method shows exceptional resilience to uncertainties and disruptions brought on by many microgrid elements. However, having an accurate model of the microgrid and carrying out the intricate calculations involved are essential for its deployment. In electrical engineering, the conventional PID controller is well-liked and often utilized [29]. Its simplicity, ease of usage, quick reaction time, and stability while regulating the microgrid's frequency are the major reasons for its appeal. Several controllers have been used to adjust frequency and improve stability in the context of islanded microgrids [29–36]. PI controllers [29, 30], PID controllers [31], PID controllers implemented using the ZN method [32], PID controllers made with GA [33], PID controllers made with PSO [34], PID controllers made with BBO [35], and PID controllers made with QOH [36] are the controllers used in this study. Although the standard PID controller only has one degree of freedom, the traditional FOPID controller offers two. Its use has several benefits, including increased precision, enhanced stability, and robust performance even in systems impacted by parameter uncertainties and disruptions [37]. As explained in [38, 39], the FOPID controller was used to efficiently regulate the microgrid's frequency regulation. Moreover, other research [40], [41], and [42], showed how different optimization strategies applied to the FOPID controller's parameters improved the performance and stability of the islanded microgrid's frequency. Specifically, a neural network was used for parameter tuning in one study, while other studies employed optimization methods such as SWA [40], SCA [41], and HSA [42]. These advancements exemplify significant contributions towards improving frequency stability within the microgrid system. In system control, it has been demonstrated that cascaded controllers perform better than single controllers such as PID and FOPID [43–45]. In order to improve frequency in power systems, the [43] uses DSA to optimize a FOPI-FOPD controller's

characteristics. Similarly, by adjusting its settings using the chaotic BOT, the PI-TID controller was utilized in [44] to improve frequency management in the microgrid. Additionally, by using the GOT to optimize its settings, the PI-FOPID controller was used in [45] to increase frequency in islanded microgrids.

Although the control methods considered for controlling VIC in islanded microgrids have improved frequency stability, they have not been resistant to severe disturbances (disruptions of load and distributed generation sources) and also to the uncertainty of islanded microgrid parameters [16-42]. Severe disturbances and uncertainties in islanded microgrids have made the performance of the VIC difficult. Therefore, there is a need to design a suitable control method for the VIC that can be resistant to these severe disturbances and uncertainties.

In the paper, a new method named PD-FOPID cascaded controller is put forward by the authors to boost the efficacy of VIC applied in microgrid. The parameters of this controller are meticulously fine-tuned using the ROA. A prominent reason for incorporating the PD-FOPID cascaded controller into the structure of VIC, instead of alternative cascaded controllers like PI-FOPID, is its ability to deliver more precise and rapid responses to variations in frequency within islanded microgrids. This attribute empowers VIC to exhibit superior performance when confronted with load disruptions, fluctuations in renewable energy sources, and uncertainties pertaining to microgrid parameters. Within the architecture of VIC, ROA assumes responsibility for optimizing various settings associated with the cascaded controller. Owing to a myriad of advantages offered by this method over other metaheuristic algorithms such as PSO, GA, GWO, and ABC, users can enjoy enhanced accuracy, expedited convergence rate, reduced parameter requirements, and improved capacity to augment solutions. The paper presents several noteworthy advancements and contributions. Firstly, the utilization of PD-FOPID cascaded controller results in improved VIC and FR within islanded microgrids. This approach represents a significant departure from previous methods. Additionally, the introduction of an ROA (which has not previously been employed in the context of VIC) allows for the optimization of suggested controller settings (PD-FOPID). The inclusion of this optimization technique enhances the precision and effectiveness of the proposed controllers. Furthermore, a thorough evaluation is conducted to assess the performance of this novel approach compared to various algorithms such as PSO, GA, GWO, and ABC for PD-FOPID controller parameter optimization. The evaluation takes into consideration important objective functions (IAE and ITAE) resulting in comprehensive insights into controller efficacy. Lastly, performance testing is undertaken on the ROA-PD-FOPID suggested controller with aims to enhance VIC performance under conditions involving disruptions and uncertainties within isolated microgrid parameters. This rigorous testing ensures that any implemented solution is capable of operating robustly under challenging circumstances.

The key contributions of this paper are as follows:

- Introduction of the PD-FOPID Controller as Part of the VIC Framework:
- Designing of the Rain Optimization Algorithm (ROA) for Parameter Tuning:
- Comprehensive Evaluation of the PD-FOPID Controller Compared to Other Metaheuristic Algorithms:
- Improved Performance of VIC and Frequency Regulation (FR) in Islanded Microgrids:
- Introduction of a Novel Application for ROA in VIC.

The forthcoming content of the paper is divided into various segments: Section 2 delves into an exploration of the investigated microgrid. In Section 3, our attention turns towards sketching the proposed controller in order to accomplish a desired VIC within the framework of said islanded microgrid structure. Moving ahead, a presentation of simulation outcomes and subsequent discussions ensue in Section 4. Ultimately, concluding thoughts are offered in Section 5.

2 The investigated microgrid

In this part, we shall discuss the various components of the investigated islanded microgrid as well as delve into the dynamic model of said microgrid.

2.1 The various components of the investigated microgrid

The structure of the studied islanded microgrid is shown in Fig. 1 [17-19]. This microgrid consists of a thermal power plant boasting a capacity of 12 MW, a WT capable of producing 7 MW, a PV system with an output potential of 9 MW, loads able to handle up to 15 MW, and lastly an energy storage resource equipped with a capacity reaching 4 MW. Collectively, these aforementioned elements constitute the foundation upon which our islanded microgrid operates [17-19]. Within this specific realm we encounter what is known as VIC-our LFC system. Implemented on our energy storage resources within this intricate setup - it serves to function as a compensator aimed towards achieving balance amidst both generation and consumption factors [17-19].

2.2 The model used to analyze the behavior of the microgrid under study

As seen in Fig. 2, a dynamic model pertaining to the microgrid under study is examined. The microgrid is thoroughly analyzed in this model [18–20]. This system's thermal power plant consists of a turbine with a dead-band governor and limiter. The lowest and maximum values of the steam valve's opening and closing speeds are denoted by VL and Vu, respectively [18–20]. The dynamic model of the microgrid has a hierarchical control framework to guarantee appropriate frequency management. The VIC loop, SC loop, and PC loop are the three separate control loops that make up the controller's structure. A droop coefficient of 1/R is incorporated into the primary control loop to provide stability [18–20]. Furthermore, the SC loop contains both an integrator controller as well as a control error system with its corresponding gain KI [21]. The microgrid being studied requires a common electrical system for frequency regulation that includes a transferring function of first-order. This function incorporates both a damping constant, D, and an inertia, H, to ensure proper balancing of the microgrid. WT systems and PV systems exemplify renewable energy sources, portrayed as first-order transfer functions with fortuitous inputs [21]. As depicted in Fig. 2, the proposed controller (ROA-PD-FOPID) is employed within the VIC structure to augment the resilience of the self-sustained microgrid and uplift frequency steadiness. Table 1 presents the parameters associated with the microgrid [17-19].
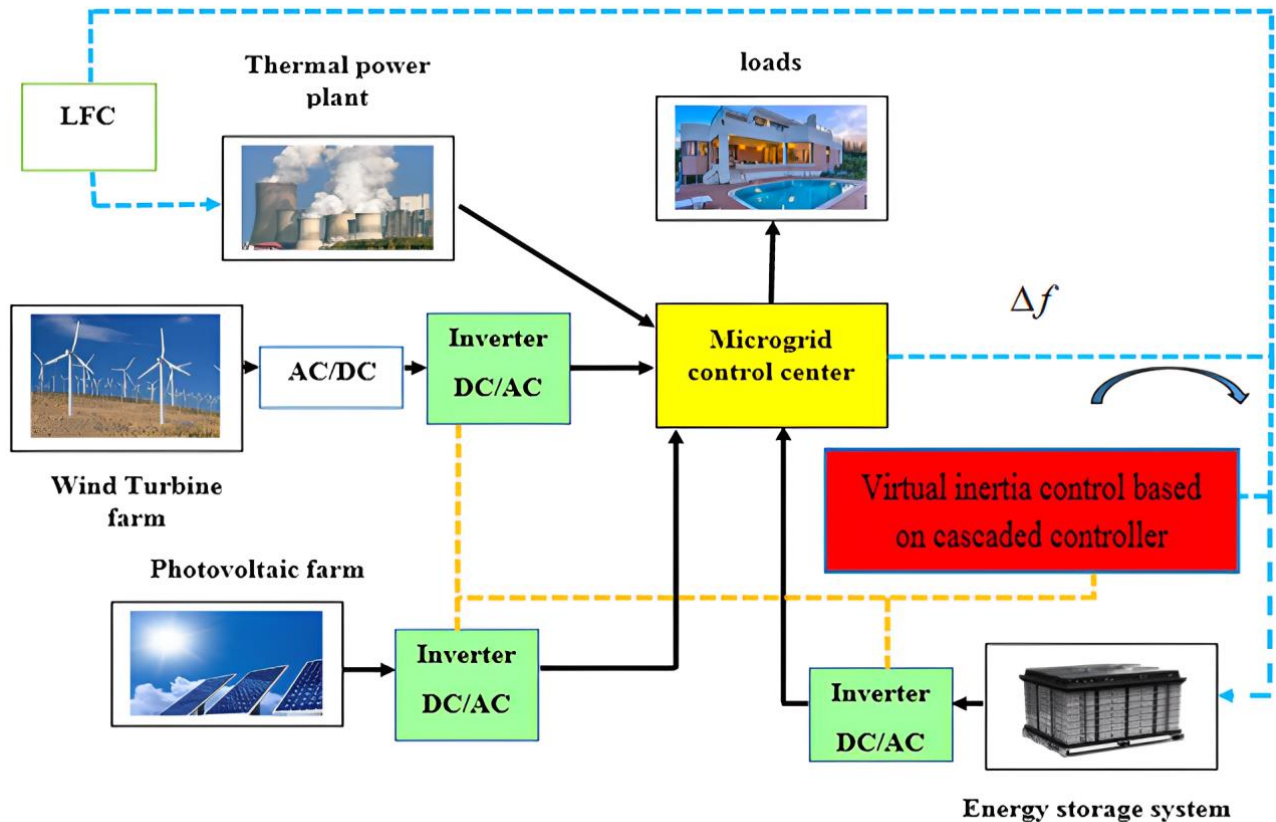

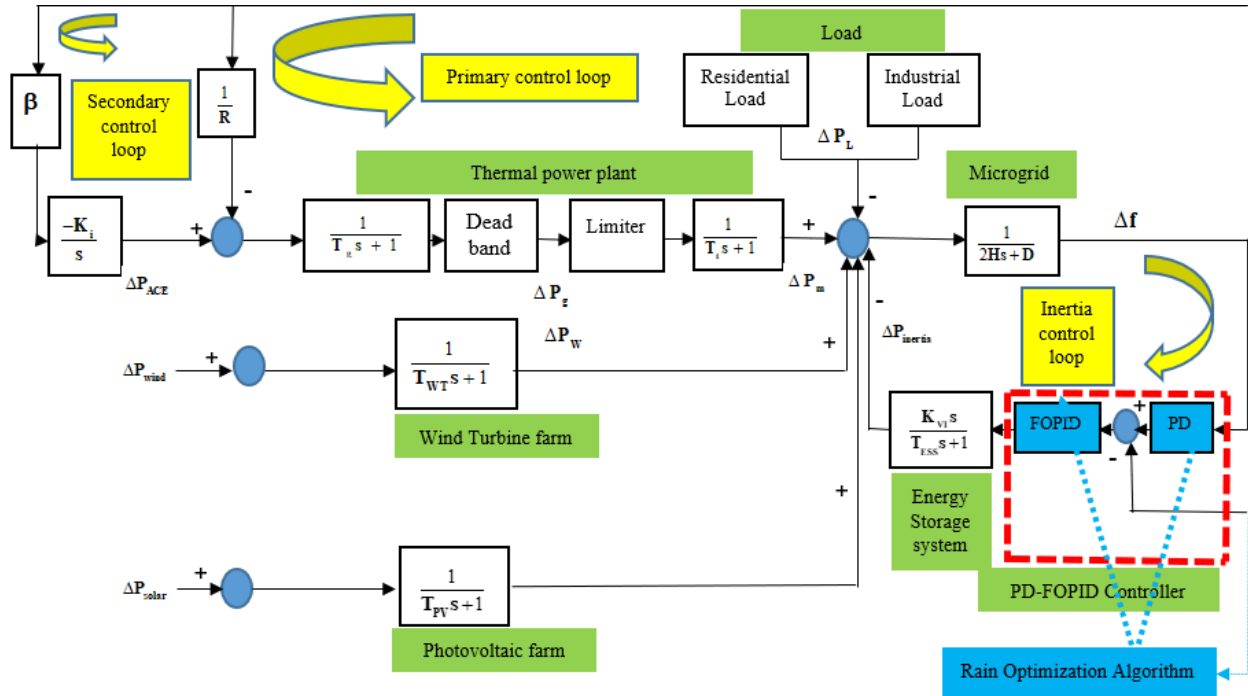**Fig. 1** The structure of the studied islanded microgrid [17-19].

Fig. 2 The dynamic model related to the studied microgrid

Table 1. The parameters associated with the microgrid [17-19]

parameter	value	parameter	value
$T_{WT}(s)$	1.50	B(pu.MW/Hz)	1
V_U(pu.MW)	0.30	$T_{ESS}(s)$	10
$T_g(s)$	0.10	D(pu.MW/Hz)	0.0151
$T_t(s)$	0.40	$K_i(s)$	0.051
$T_{PV}(s)$	1.80	R(Hz/pu.MW)	2.42
$K_{VI}(s)$	0.50	H(pu.MW/Hz)	0.0833
V_L(pu.MW)	-0.30		

3 The formulation of the controller intended to achieve the desired performance of the VIC in the microgrid structure.

This section discusses the proposed controller's structure, the analysis of the ROA, and the plan of the controller using the ROA.

3.1 The proposed controller

The PD-FOPID controller that is used in cascaded form has dual benefits - it can reduce the effects of disturbances and uncertain factors in the VIC structure which cause frequency deviations, and also enhance the inertia of the isolated microgrid. There are two controllers in the proposed control mechanism - the PD controller and the FOPID controller. The set-point of the

FOPID controller is regulated by the output of the PD controller. Within this configuration, the PD controller assumes a primary or external role, whereas the FOPID controller functions as a secondary or internal entity. Fig. 3 illustrates how the recommended PD-FOPID controller for VIC in a microgrid is structured, with equation (1) representing its transfer function within the inner loop.
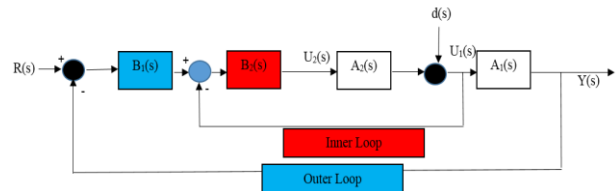

Fig. 3 The recommended PD-FOPID controller for VIC in the studied system

$$Y_2(s) = A_2(s)U_2(s) \tag{1}$$

In equation (1), $A_2(s)$ is the transfer function of the internal process, and $U_2(s)$ is the process's input signal. With $A1(s)$ denoting the inner loop's output and $U_1(s)$ denoting the reference signal, equation (2) illustrates the outer loop's transfer function. The PD controller in the outer layer is represented by $B_1(s)$ in Fig. 3, while the FOPID controller in the inner layer is represented by $B_2(s)$. Equations (3) and (4) provide the transfer functions for the PD and FOPID controllers, respectively. The controller's whole internal structure is shown in Fig. 4.

$$Y(s) = A_1(s)U_1(s) + d(s) \tag{2}$$

$$B_1(s) = K_{P1} + K_{d1}s \tag{3}$$

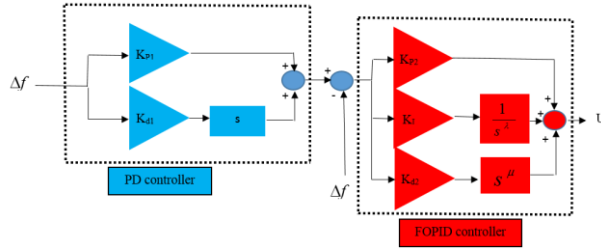$$B_2(s) = K_{P2} + K_I s^{-\lambda} + K_{d2}s^{\mu} \tag{4}$$

Fig. 4 The complete internal structure of the controller

In order to minimize two different objective functions, IAE and ITAE, the recommended settings for this controller were obtained by applying the Rain optimization algorithm (ROA). Equations (5) and (6) respectively reflect these goal functions. To shed further light on these objective functions, the restrictions are illustrated using equations (7) to (13).

$$IAE = \int_0^{t_s} |\Delta f|\, dt \tag{5}$$

$$ITAE = \int_0^{t_s} |\Delta f|\, t\, dt \tag{6}$$

$$K_{P1,min} \le K_{P1} \le K_{P1,max} \tag{7}$$

$$K_{d1,min} \le K_{d1} \le K_{d1,max} \tag{8}$$

$$K_{P2,min} \le K_{P2} \le K_{P2,max} \tag{9}$$

$$K_{I,min} \le K_I \le K_{I,max} \tag{10}$$

$$K_{d2,min} \le K_{d2} \le K_{d2,max} \tag{11}$$

$$\lambda_{min} \le \lambda \le \lambda_{max} \tag{12}$$

$$\mu_{min} \le \mu \le \mu_{max} \tag{13}$$

3.2 Rain optimization algorithm (ROA)

About any optimization method such as GA, PSO, GWO, and ABC algorithm, the rain optimization technique has its advantages [46–48]:

- Simplicity: ROA is easy to implement so it is widely known. Normally all that is needed is a few basic formulas and there is no need for complicated calibration of parameters.
- Efficiency: Since ROA has the ability to efficiently exploit the promising regions of the search space, it can often be said to converge on the optimal solutions in a relatively short time. Because of this, it can be applied to tasks with a complex topology or large dimensionality of search space.
- The delicate balance between exploration and

exploitation: ROA also allows being aggressive and seeking new solutions while at the same time being conservative and using available solutions that are better. This peculiar feature prevents it from being trapped in locally optimal solutions.

- Robustness: ROA tends to exhibit robust performance across various problem domains. It can handle both continuous and discrete optimization problems, making it versatile in different application areas.
- Fewer Parameters: ROA typically requires fewer user-defined parameters compared to other optimization algorithms. This simplifies the optimization process and reduces the need for extensive parameter tuning.

Each solution to the problem possesses the characteristics of a raindrop [46]. As the raindrops descend haphazardly upon the ground, certain points within the realm of possible answers are randomly selected [47]. The defining attribute of these raindrops is their radius, which fluctuates steadily over time – diminishing as temporal progress marches on and expanding whenever a connection with another droplet is established [48]. Once an initial set of potential solutions has been established, each droplet's radius is attributed at random from within a suitable range [46]. In every subsequent iteration, individual droplets survey their surroundings in accordance with their size [46-48]. Those solitary drops that remain disconnected from any others simply acknowledge their physical boundaries without regarding external factors [46-48]. When tackling problems existing within n-dimensional space, each drop represents n variables: it is during this first stage that we examine variable one's minimum and maximum thresholds; these boundaries are determined by the respective droplet's radius [46-48]. Upon proceeding to the subsequent phase, a meticulous examination is conducted on two opposing terminations of variable two, prolonging this course until the final variable is assessed [46]. It is during this juncture that the cost function associated with the foremost droplet undergoes an amendment by descending it in position [47]. Such an act should not be misconstrued as its ultimate disposition; rather, ascertained through the gradual diminishment of the cost function, it remains steadfastly bound to its downward trajectory [47]. This operation shall be executed ubiquitously for each droplet, promulgating both their respective positions and costs collectively [48]. Furthermore, alterations shall occur twofold about the radius measurement warranted for every distinct droplet.

In the event that two minuscule droplets, each with their respective radii denoted as r_1 and r_2, find themselves in such proximity to one another that a

shared region is created between them, it becomes possible for these droplets to amalgamate and give rise to a grander entity - an enlarged droplet of radius R (equation 14) [46-48]. In equation (14), the variable "n" represents the count of variables within each droplet.

$$R = (r_1^n + r_2^n)^{\frac{1}{n}} \qquad (14)$$

If a droplet of size r1 remains stationary, the degree to which it is absorbed into the soil, as indicated by α, may vary and result in a certain proportion of its volume being adsorbed (equation 15).

$$R = (\alpha r_1^n)^{\frac{1}{n}} \qquad (15)$$

In equation (15), the symbol α denotes the proportion, expressed as a percentage, of a droplet's volume that can be assimilated during each successive iteration. This value lies within the range of 0 to 100 percent [46]. Additionally, it is possible to establish a lower limit for the radius of droplets known as r_{min}; any droplet possessing a radius smaller than r_{min} will cease to exist [47]. It is conceivable that the population size would diminish over a series of iterations, resulting in the development of larger droplets capable of exploration on a broader scale [48]. By expanding the scope of investigation for each droplet, their capacity for localized search increases in direct proportion to their diameter [47]. Consequently, as the number of iterations rises, feeble droplets with limited investigation capabilities vanish or merge with more potent drops possessing wider investigative domains [46-48]. Thus, the initial population dwindles significantly due to an accelerated pace in uncovering the correct answer(s). In essence, the initial configuration of this algorithm encompasses crucial tuning parameters [46]. These components consist of the number of raindrops at the beginning (population size), as well as the scope in which each population will search for potential solutions (raindrop radius) [47]. In the preliminary phase of the algorithm, a distinct value is bestowed upon each droplet in correspondence with its performance according to the cost function [47]. Subsequently, every individual droplet commences its downward trajectory [48]. To ensure efficacy, an evaluation by means of the cost function is made when assessing both ends of a given droplet [46-48]. Once started, the droplet always moves along its trajectory until it reaches at least one minimum point during its journey [47]. For each droplet, the same series of events unfolded. Along their way, neighboring droplets could coalesce, dramatically increasing the performance of the algorithm [47]. When a droplet reached its end, it would start to lose mass, but this allowed a significant betterment of solution accuracy [48]. With the application of this method, the algorithm

is capable of locating all the peak values in the target function [48].

3.3 The plan of the proposed controller utilizing the ROA

The VIC structure is utilized to undertake multiple stages for optimizing the control parameters of the PD-FOPID controller in an islanded microgrid using the ROA:

1) Before setting out on the path, it is crucial that we look more closely at the problem: particularly, the definition of the goal function needs to be made clearer, which comprises most importantly the minimization problems of IAE, and ITAE within the control system. It is also necessary if not more importantly, to define and express any constraints pertaining to this situation as well.

2) Initialize the population: Propose a random population of possible solutions which are the sets of the PD-FOPID parameters.

3) Evaluate the fitness: The fitness of the members of the population is assessed by IAE, and ITAE of every current member using the PD-FOPID parameters from the previous member.

4) Update the best solution: Use the better candidates from the present generation to evaluate their merits.

5) Generate new solutions: New candidate solutions are created using the new proposed candidates by using paradigm perturbation, a technique used to form new solutions from the best solutions.

6) Evaluate the fitness of new solutions: The fitness of the new solutions is worked out by evaluating IAE, and ITAE in consideration of the new set of PD-FOPID parameters.

7) Update the best solution: Whenever any fitness of the new solution is greater than the best previous fitness, perform a suitable modification to the best solution.

8) Update the population: In the current population the worst solutions are eliminated and new solutions are incorporated.

9) Repeat steps 5-8: Either for a specified number of iterations or until a termination condition is satisfied, repeat steps 5 through 8.

10) Output the best solution: A descriptive presentation and analysis of IAE, and ITAE with the best PD-FOPID parameters will be given after the algorithm termination event.

Fig. 5 shows how the ROA technique is used to optimize the PD-FOPID controller parameters in an autonomous microgrid. The process is carried out within the VIC framework.
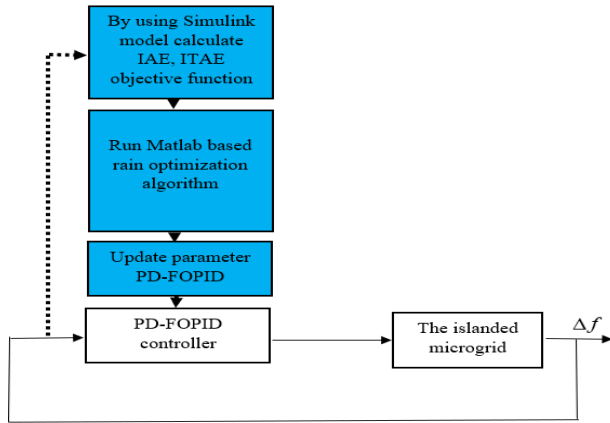
Fig. 5 The ROA technique is used to optimize the PD-FOPID controller parameters

Implementing the proposed method in a real environment may entail several challenges, including:

- Computational complexity and convergence time: Implementing the ROA algorithm and fine-tuning the controller parameters can require complex and time-consuming calculations.
- Sensitivity to initial settings: The initial settings of the controller and the optimization algorithm may affect the final performance and require different experiments that must be tested under different conditions, and this is why several different scenarios are used in this paper.
- Cost and complexity of implementation: Implementing advanced algorithms in a real environment may be costly and require high technical expertise.

4 Simulation Results and Discussion

In this specific portion, different scenarios have been simulated to assess the islanded microgrid. In the first scenario, there are two segments. The first segment assesses the performance and convergence of the ROA algorithm in optimizing the parameters of the PD-FOPID controller. It also compares the ROA algorithm's performance with other algorithms such as PSO, GWO, GA, and ABC. Secondly, comparing the proposed ROA-PD-FOPID controller with numerous methods such as controllers 1 to 6 and in the studied system during load disruptions. In scenario (2), the proposed method is subjected to a comparative analysis alongside various other methods including controllers 1 to 6 in the studied system. This analysis evaluates how well they perform when faced with load disruptions and uncertainties related to the parameters of the system. The effectiveness of the proposed method in managing load disruptions, interruptions in renewable energy sources, and minor uncertainties in the system's parameters are evaluated and compared to other methods in the scenario

(3). Scenario (4) involves comparing the proposed method's performance with other methods in terms of its capability to handle load disruptions, interruptions in WT, and significant uncertainties in the studied system's parameters.

4.1 Scenario (1)

Within this particular scenario, a disruption of $\Delta PL=0.1pu$ seamlessly integrates with the autonomous microgrid at t=1 seconds, as evident in Fig. 6. Table 2 provides the initial parameters for both the PD-FOPID and the ROA. Fig. 7 serves to depict the progression of various algorithms such as ROA, GA, PSO, GWO, and ABC in their endeavor to optimize the PD-FOPID controller parameters whilst focusing on minimizing IAE. Taking into account Fig. 7's data, it is clear that the ROA algorithm showcases a more rapid convergence rate than its counterparts. Furthermore, the IAE values achieved by each algorithm are as follows: ROA - 0.0023, GWO - 0.0027, GA - 0.0028, ABC - 0.0033, and PSO - 0.0036 respectively. The optimized parameters of the PD-FOPID controller can be seen in Table 3, utilizing several optimization algorithms, namely ROA, GWO, GA, ABC, and PSO. The IAE and ITAE are taken into consideration as the objective functions. Based on the results presented in Fig. 7 and Table 3, it was concluded that the ROA algorithm is the most effective method for optimizing the parameters of the PD-FOPID controller and will be used in this scenario. This scenario involves applying a disturbance to the microgrid, which is shown in Fig. 6. The objective is to maximize the efficiency of the PD-FOPID controller under these conditions. The applied signal generated by the proposed controller for this microgrid can be observed in Fig. 8. Additionally, Figs 9. a and 9.b exhibit FR of the system employing various control strategies. To further analyze Scenario (1), referring to Table 4 presents results from different control methods utilized in this Scenario. Based on the data provided in Table 4, it is observed that the proposed method employing a VIC based on a ROA-PD-FOPID controller yields an MFD of 0.0071 Hz and ST of 0.172 seconds. The MFD and ST using controller 1 are 0.0391 Hz and 0.542 seconds, respectively. The MFD and ST using the controller 2 are 0.0763 Hz and 14.625 seconds, respectively. The MFD and ST using controller 3 are 0.127 Hz and 24.65 seconds, respectively. The MFD and ST using controller 4 are 0.183 Hz and 17.795 seconds, respectively. The MFD and ST using controller 5 are 0.256 Hz and 26.417 seconds, respectively. The MFD and ST without using controller 6 are 0.345 Hz and 21.56 seconds, respectively. Concurring with the outcome of scenario (1), the proposed strategy has illustrated palatable execution compared to other utilized

strategies in moderating the impacts of stack disturbances, altogether lessening recurrence deviations caused by stack disturbance. Also, the ST related to recurrence deviations caused by stack disruption has been quickened utilizing the proposed strategy.
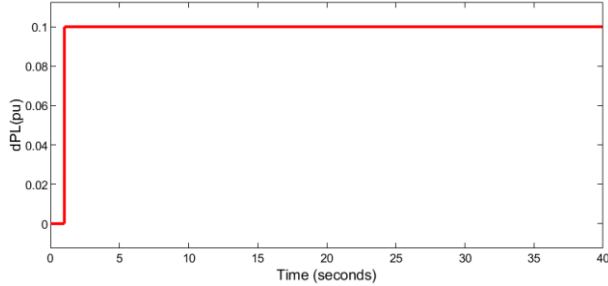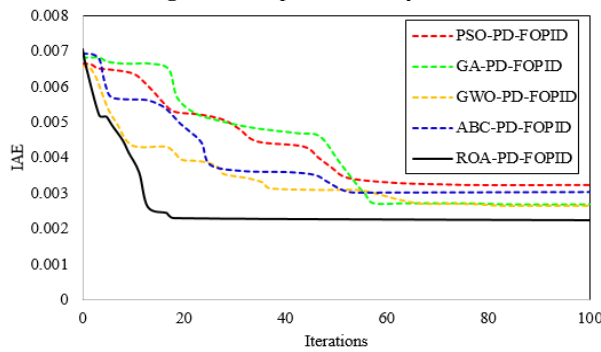

Fig. 6 A disruption of the system

Fig. 7 The progression of various algorithms such as ROA, ABC, GWO, GA, and PSO in their endeavor to optimize the PD-FOPID controller parameters whilst focusing on minimizing IAE

Table 2. The parameters for both the PD-FOPID and the ROA

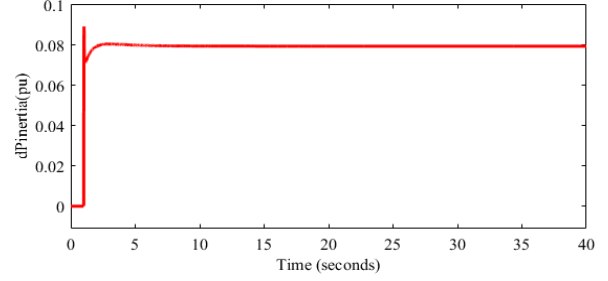| parameter	value	parameter	value
Variables number of each raindrop	2	$K_{P1,min}, K_{d1,min},$ $K_{P2,min}, K_{I,min}, K_{d2,min}$	0
Initial raindrops diameter	0.036	$K_{P1,max}, K_{d1,max},$ $K_{P2,max}, K_{I,max}, K_{d2,max}$	100
Initial raindrops number	100	λ_{min}, μ_{min}	0
maxIterations	100	λ_{max}, μ_{max}	1

Fig. 8 The signal generated by the proposed controller, Scenario (1)
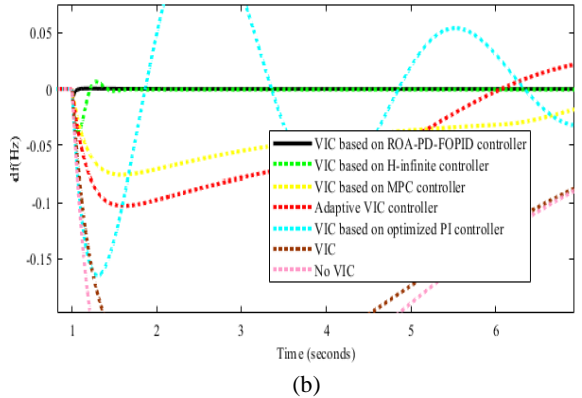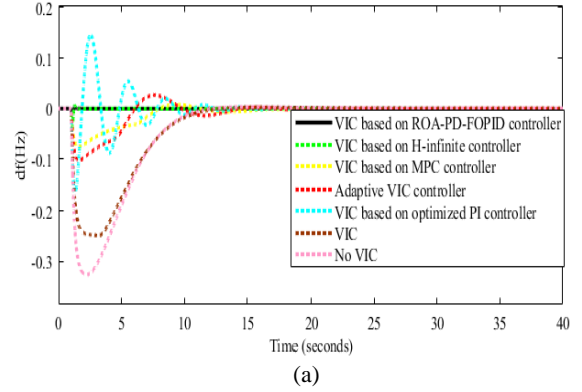

(a)

(b)

Fig. 9. (a) The FR of the system, Scenario (1).(b) The FR of the system, Scenario (1)

Table 3. The best settings for the PD-FOPID controller have been found using different optimization methods like ROA, GWO, GA, ABC, and PSO.

Controller	K_{P1}	K_{d1}	K_{P2}	K_I	K_{d2}	λ	μ	IAE	ITAE
ROA-PD-FOPID	95.36	91.85	87.97	97.91	88.48	0.396	0.23	0.0023	0.0089
GWO-PD-FOPID	90.76	86.01	94.42	90.53	87.01	0.284	0.18	0.0027	0.0106
GA-PD-FOPID	89.49	86.55	91.33	91.66	79.23	0.387	0.07	0.0028	0.0113
ABC-PD-FOPID	73.99	91.11	87.66	74.24	80.42	0.426	0.31	0.0033	0.0154
PSO-PD-FOPID	70.27	84.98	74.21	78.76	82.86	0.231	0.09	0.0036	0.0157

Table 4. The MFD and ST associated with frequency deviation utilizing various control strategies, Scenario (1)

Controller	MFD (Hz)	ST(sec)
VIC based on ROA-PD-FOPID controller	0.0071	0.172
Controller 1	0.0391	0.542
Controller 2	0.0763	14.625
Controller 3	0.127	24.65
Controller 4	0.183	17.795
Controller 5	0.256	26.417
Controller 6	0.345	21.56

Fig. 10 The signal generated by the proposed controller, Scenario (2)

4.2 Scenario (2)

In this scenario, a stack disturbance has been presented to the system, taking under consideration the instability related with the parameters (H = -50%). The applied signal generated by the proposed controller for this microgrid can be observed in Fig. 10. Figs. 11. a and 11. b illustrate the FR of the system with different control strategies, and Table 5 displays the results obtained from various control strategies in scenario (2). According to Table 5, the MFD and ST using the proposed method are 0.0087 Hz and 0.189 seconds, respectively. The MFD and ST using controller 1 are 0.053 Hz and 0.77 seconds, respectively. The MFD and ST using controller 2 are 0.10 Hz and 23.81 seconds, respectively. The MFD and ST using controller 3 are 0.146 Hz and 26.07 seconds, respectively. The MFD and ST using controller 4 are 0.21 Hz and 22.16 seconds, respectively. The MFD and ST using controller 5 are 0.38 Hz and 29.85 seconds, respectively. The MFD and ST using the controller 6 are 0.43 Hz and 22.78 seconds, respectively. In light of the findings from scenario (2), the method put forth has demonstrated commendable effectiveness when juxtaposed with alternative methods employed in addressing disturbances and uncertainties tied to system parameters. It has proven particularly adept at diminishing frequency deviations induced by load disruptions, thereby mitigating their impact significantly. Furthermore, the proposed method has effectively expedited the ST associated with frequency deviations emanating from load disruptions and uncertainties stemming from system parameters.
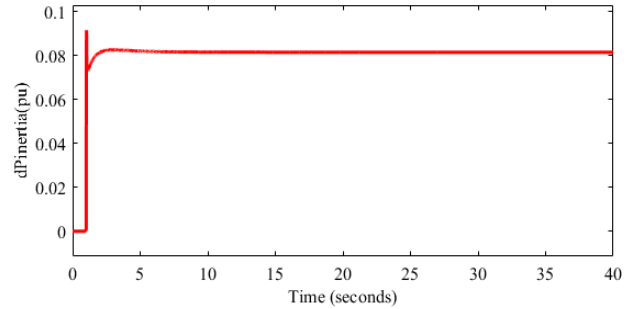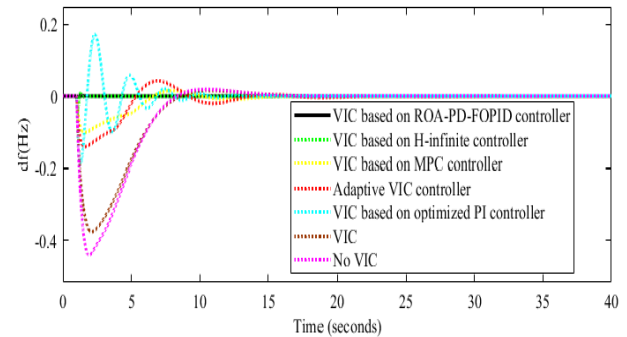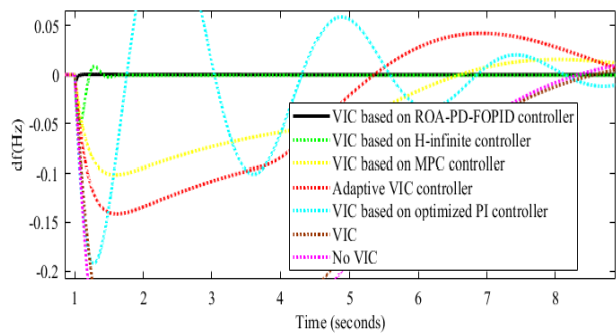

(a)

(b)

Fig. 11. (a) The FR of the system, Scenario (2).(b) The FR of the system, Scenario (2)

Table 5. The MFD and ST associated with frequency deviation using various control strategies, Scenario (2)

Controller	MFD (Hz)	ST(sec)
VIC based on ROA-PD-FOPID controller	0.0087	0.189
Controller 1	0.053	0.77
Controller 2	0.10	23.81
Controller 3	0.146	26.07
Controller 4	0.21	22.16
Controller 5	0.38	29.85
Controller 6	0.43	22.78

4.3 Scenario (3)

Fig. 12 presents a scenario where the system experiences both load disruptions and disruptions in WT. Moreover, a slight level of uncertainty (H=-5%) is taken into account for the microgrid parameters within this particular setting. The figure below portrays the signal applied by the proposed controller to operate the system (Figure 13). In Fig. 14. a, 14.b, and 14.c, the FR of the system using various control strategies is shown. Table 6 summarizes the outcomes of different control strategies applied for scenario (3). The proposed method using MFD yields a value of 0.0028 Hz. The MFD using controller 1 is 0.053 Hz. The MFD using controller 2 is 0.266 Hz. The MFD using controller 3 is 0.331 Hz. The MFD using controller 4 is 0.389 Hz. The MFD using controller 5 is 0.717 Hz. The MFD using controller 6 is 0.806 Hz. Concurring with the comes about of scenario (3), the proposed strategy has performed well compared to other strategies in relieving the recurrence deviations caused by stack disturbances, renewable vitality source disturbances, and slight instability in framework parameters.
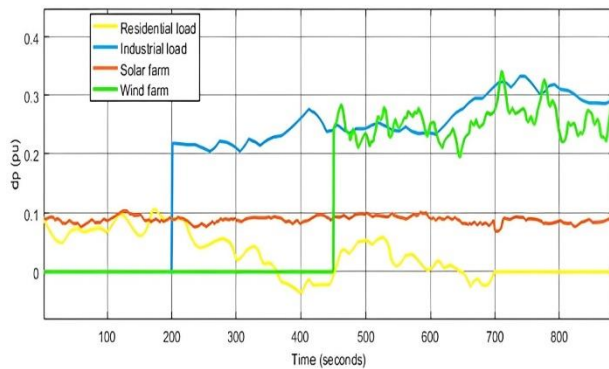

Fig. 12 The disruptions in both load and renewable energy sources are imposed on the microgrid, Scenario (3)
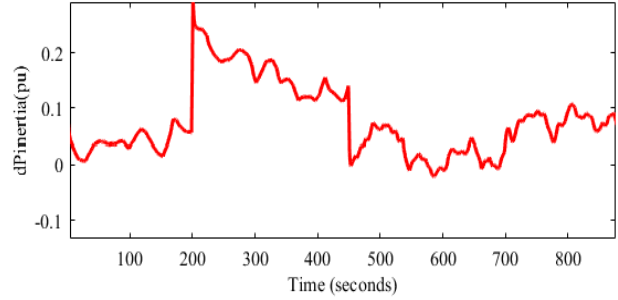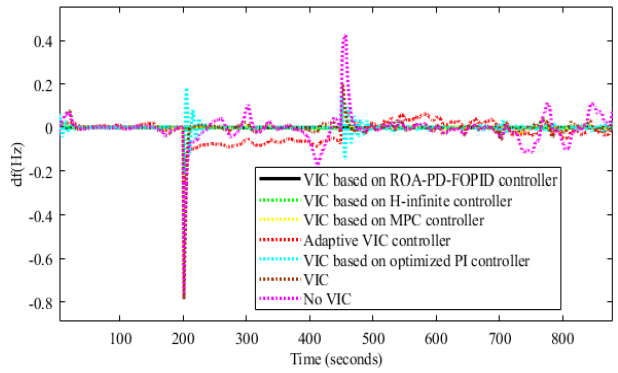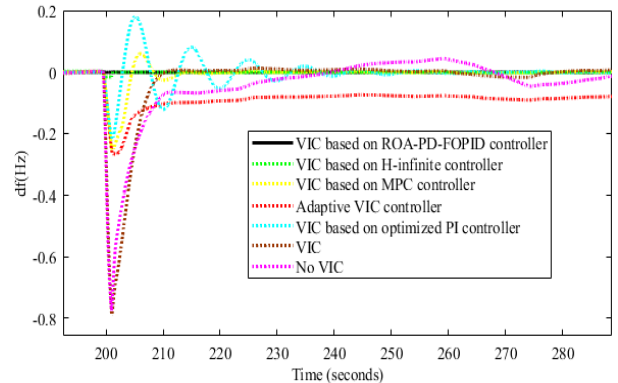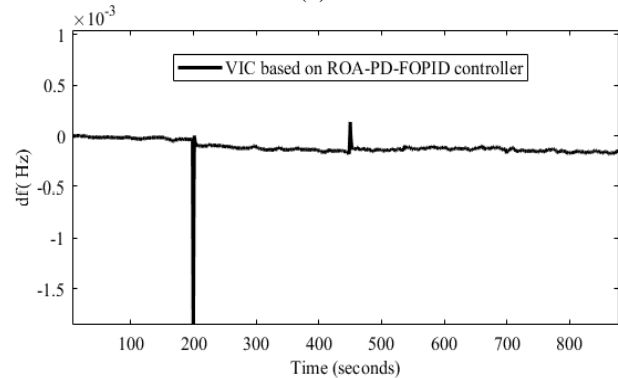

Fig. 13 The signal generated by the proposed controller, Scenario (3)

(a)

(b)

(c)

Fig. 14. (a) The FR of the system, Scenario (3).(b) The FR of the system, Scenario (3).(c) The FR of the system, Scenario (3)

Table 6. The MFD using various control strategies, Scenario (3)

Controller	MFD(Hz)
VIC based on ROA-PD-FOPID controller	0.0028
Controller 1	0.053
Controller 2	0.266
Controller 3	0.331
Controller 4	0.389
Controller 5	0.717
Controller 6	0.806

4.4 Scenario (4)

The microgrid in Figure 12 is subjected to both stack disturbances and disturbances from renewable energy sources. In this situation, noteworthy instability within the microgrid parameters ((T_g=+50%, H=-85%, T_t=+90%) is additionally considered. Fig. 15 showcases the signal implemented by the proposed controller to the system. In Figs. 16. a, 16.b, and 16.c, the FR of the system using various control strategies is depicted. Table 7 displays the outcomes of different control approaches employed in scenario (4). According to Table 7, The MFD using the proposed method is 0.0031 Hz. The MFD using controller 1 is 0.064 Hz. The MFD using controller 2 is 0.46 Hz. The MFD using controller 3 is 0.51 Hz. The MFD using controller 4 is 0.72 Hz. The MFD using controller 5 is 2.3 Hz. The MFD controller 6 is 2.7 Hz. Concurring with the outcome of scenario (4), the proposed strategy has appeared alluring execution compared to other utilized strategies against stack disturbances, renewable vitality sources disturbances, and critical vulnerability in framework parameters, altogether decreasing recurrence deviations caused by stack disturbances.
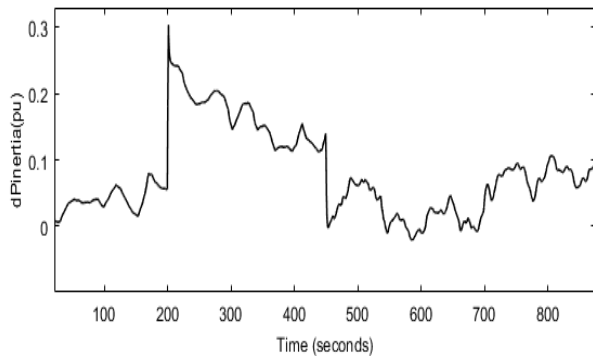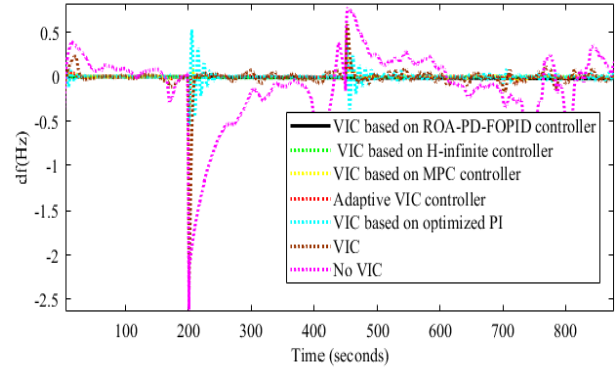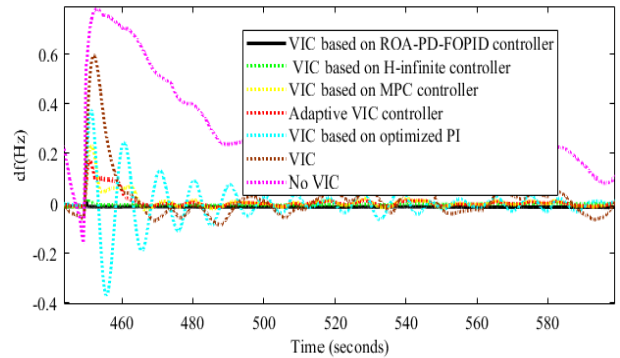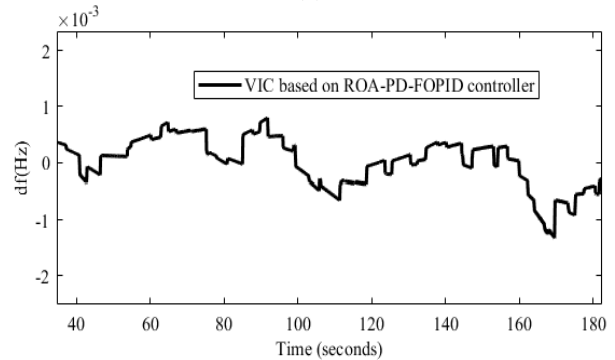

Fig. 15 The signal generated by the proposed controller, Scenario (4)

(a)

(b)

(c)

Fig. 16. (a) The FR of the system, Scenario (4).(b) The FR of the system, Scenario (4).(c) The FR of the system, Scenario (4)

Table 7. The MFD using the various control methods, Scenario (4)

Controller	MFD (Hz)
VIC based on ROA-PD-FOPID controller	0.0031
Controller 1	0.064
Controller 2	0.46
Controller 3	0.51
Controller 4	0.72
Controller 5	2.3
Controller 6	2.7

5 Conclusion

In this paper, a novel and robust approach for enhancing VIC performance in islanded microgrids was developed, introducing the PD-FOPID cascaded controller optimized using the ROA. The proposed approach demonstrates remarkable advancements in addressing challenges posed by load disturbances, renewable energy source fluctuations, and uncertainties in microgrid parameters. Compared to other metaheuristic algorithms such as PSO, GA, GWO, and ABC, the ROA proved highly effective in optimizing the PD-FOPID controller's parameters, offering superior convergence speed, enhanced accuracy, reduced complexity, and fewer parameter requirements. The evaluations showed that the ROA-PD-FOPID controller significantly outperformed six alternative control strategies across various scenarios. The proposed controller (ROA-PD-FOPID)

reduced MFD by up to 95% and ST by up to 76% compared to conventional methods under complex and challenging scenarios. The ROA-PD-FOPID effectively mitigated frequency deviations caused by uncertainties and parameter variations, ensuring reliable performance even under extreme conditions. Unlike traditional methods, the ROA-PD-FOPID controller rapidly responded to changes in system dynamics, maintaining robust frequency regulation in islanded microgrids. The use of the ROA in this context represents a significant step forward in VIC optimization, providing a practical and scalable solution for real-world applications. By addressing the limitations of existing approaches, such as dependency on accurate models and limited robustness under uncertainties, this method bridges critical gaps in microgrid frequency control.

NOMENCLATURE:

ABC	Artificial bee colony	SWA	Salp swarm algorithm
BBO	Biogeography-based optimization	SC	Secondary control
BOT	Butterfly optimization technique	ST	Settling time
DSA	Dragonfly search algorithm	VIC	Virtual inertia control
FOPID	Fractional order PID	ΔP_L	Load Variations
FR	Frequency response	Δf	Frequency Variations
GA	Genetic Algorithm	T_{ESS}	Time Constant of Energy Storage System
GTO	Gorilla troops optimizer	ΔP_m	Thermal Power Plant Generated Power Variations
GWO	Grey wolf optimizer	ΔP_g	Governor Power Variations
HSA	harmony search algorithm	ΔP_{ACE}	Control Signal for Secondary Contro
IAE	Integral absolute error	T_{PV}	Time Constant of Photovoltaic System
ITAE	Integral time absolute error	T_{WT}	Time Constant of Wind Turbine
MPC	Model predictive control	T_t	Time Constant of Thermal Power Plant Turbine
MFD	Maximum frequency deviation	T_g	Time Constant of Governor
PSO	Particle swarm optimization	ΔP_{solar}	Photovoltaic Power Variations
PC	Primary control	K_{VI}	Gain for Virtual Inertia Contro
QOH	Quasi-oppositional harmony search algorithm	ΔP_{wind}	Wind Turbine Power Variations
ROA	Rain optimization algorithm	RPWFNN	Recyrrent probabilistic wavelet fuzzy neural network
SCA	Sine cosine algorithm	PV	Photovoltaic
SG	Synchronous generators	WT	Wind Turbine
		ZN	Ziegler-Nichols

References

[1] M. Dodangeh, N. Ghaffarzadeh, "An Intelligent Machine Learning-Based Protection of AC Microgrids Using Dynamic Mode Decomposition," Iranian Journal of Electrical & Electronic Engineering, vol. 18, no. 4, 2022.

[2] F. Amiri, M. H. Moradi, "Coordinated Control of LFC and SMES in the Power System Using a New Robust Controller," Iranian Journal of Electrical & Electronic Engineering, vol. 17, no. 4, 2021.

[3] P. B. Nempu, J. N. Sabhahit, "A New Power Management Approach for PV-Wind-Fuel Cell Hybrid System in Hybrid AC-DC Microgrid Configuration," Iranian Journal of Electrical and Electronic Engineering, vol. 16, no. 4, pp. 2020.

[4] F. Amiri, M. H. Moradi, "Design of a new control method for dynamic control of the two-area microgrid," Soft Computing, vol. 27, no. 10, pp. 6727–6747, 2023.

[5] F. Amiri, M. H. Moradi, "Improving the MPC performance of the model in order to improve the frequency stability of the two-area microgrid," International Journal of Industrial Electronics Control and Optimization, 2024.

[6] F. Amiri, "Virtual Inertia Control in a Two-Area Microgrid Using Linear Matrix Inequality," Journal of Nonlinear Systems in Electrical Engineering, vol. 9, no. 2, pp. 85–115, 2023.

[7] F. Amiri, M. H. Moradi, M. Eskandari, "Suppression of low- frequency oscillations in hybrid/multi microgrid systems with an improved model predictive controller," IET Renewable Power Generation, 2024.

[8] F. Amiri, A. Hatami, "Load frequency control for two-area hybrid microgrids using model predictive control optimized by grey wolf-pattern search algorithm," Soft Computing, vol. 27, no. 23, pp. 18227–18243, 2023.

[9] F. Amiri, A. Hatami, "Load Frequency Control Via Adaptive Fuzzy PID Controller In An Isolated Microgrid," in 32nd International Power System Conference, Oct. 2017.

[10] N. S. Hasan, N. Rosmin, N. M. Nordin, S. Abd Bakar, A. H. M. Aman, "Dynamic response of hybrid energy storage-based virtual inertial support in wind application," Journal of Energy Storage, vol. 53, pp. 105181, 2022.

[11] H. Abbou, S. Arif, A. Delassi, "Frequency Enhancement of Power System with High Renewable Energy Penetration Using Virtual Inertia Control Based ESS and SMES," in International Conference on Artificial Intelligence in Renewable Energetic Systems, Nov. 2022, pp. 602–613.

[12] T. Kerdphol, F. S. Rahman, V. Phunpeng, M. Watanabe, Y. Mitani, "Demonstration of virtual inertia emulation using energy storage systems to support community-based high renewable energy penetration," in 2018 IEEE Global Humanitarian Technology Conference (GHTC), pp. 1–7, 2018.

[13] V. Skiparev, J. Belikov, E. Petlenkov, Y. Levron, "Reinforcement learning-based MIMO controller for virtual inertia control in isolated microgrids," in 2022 IEEE PES Innovative Smart Grid Technologies Conference Europe (ISGT-Europe), pp. 1–5, 2022.

[14] W. Zeng, J. Xiong, Z. Qi, "DCNN-based virtual synchronous generator control to improve frequency stability of PV-ESS station," in 2022 12th International Conference on CYBER Technology in Automation, Control, and Intelligent Systems (CYBER), pp. 861–865, 2022.

[15] B. Long, W. Zeng, J. Rodríguez, C. Garcia, J. M. Guerrero, K. T. Chong, "Stability Enhancement of Battery-Testing DC Microgrid: An ADRC-Based Virtual Inertia Control Approach," IEEE Transactions on Smart Grid, vol. 13, no. 6, pp. 4256–4268, 2022.

[16] Y. Hu, W. Wei, Y. Peng, J. Lei, "Fuzzy virtual inertia control for virtual synchronous generator," in 2016 35th Chinese Control Conference (CCC), pp. 8523–8527, 2016.

[17] K. Mentesidi, R. Garde, M. Aguado, E. Rikos, "Implementation of a fuzzy logic controller for virtual inertia emulation," in 2015 International Symposium on Smart Electric Distribution Systems and Technologies (EDST), pp. 606–611, 2015.

[18] T. Kerdphol, F. S. Rahman, Y. Mitani, K. Hongesombut, S. Küfeoğlu, "Virtual inertia control-based model predictive control for microgrid frequency stabilization considering high renewable energy integration," Sustainability, vol. 9, no. 5, pp. 773, 2017.

[19] A. Saleh, H. M. Hasanien, R. A. Turky, B. Turdybek, M. Alharbi, F. Jurado, W. A. Omran, "Optimal Model Predictive Control for Virtual Inertia Control of Autonomous Microgrids," Sustainability, vol. 15, no. 6, pp. 5009–xx, 2023.

[20] B. Long, W. Zeng, J. Rodríguez, J. M. Guerrero, K. T. Chong, "Voltage regulation enhancement of DC-MG based on power accumulator battery test system: MPC-controlled virtual inertia approach," IEEE Transactions on Smart Grid, vol. 13, no. 1, pp. 71–81, 2021.

[21] T. Kerdphol, F. S. Rahman, Y. Mitani, M. Watanabe, S. K. Küfeoğlu, "Robust virtual inertia control of an islanded microgrid considering high penetration of renewable energy," IEEE Access, vol. 6, pp. 625–636, 2017.

[22] T. Kerdphol, F. S. Rahman, M. Watanabe, Y. Mitani, "Robust Virtual Inertia Control of a Low Inertia Microgrid Considering Frequency Measurement Effects," IEEE Access, vol. 7, pp. 57550–57560, 2019.

[23] J. Li, B. Wen, H. Wang, "Adaptive virtual inertia control strategy of VSG for micro-grid based on improved bang-bang control strategy," IEEE Access, vol. 7, pp. 39509–39514, 2019.

[24] H. Ali, G. Magdy, B. Li, G. Shabib, A. A. Elbaset, D. Xu, Y. Mitani, "A new frequency control strategy in an islanded microgrid using virtual inertia control-based coefficient diagram method," IEEE Access, vol. 7, pp. 16979–16990, 2019.

[25] A. Karimipouya, S. Karimi, H. Abdi, "Microgrid frequency control using the virtual inertia and ANFIS-based Controller," International Journal of Industrial Electronics, Control and Optimization, vol. 2, no. 2, pp. 145–154, 2019.

[26] K. H. Tan, F. J. Lin, C. M. Shih, C. N. Kuo, "Intelligent Control of Microgrid with Virtual Inertia Using Recurrent Probabilistic Wavelet Fuzzy Neural Network," IEEE Transactions on Power Electronics, 2019.

[27] F. Amiri, M. Moradi, "Designing a new robust control for virtual inertia control in the microgrid with regard to virtual damping," Journal of Electrical and Computer Engineering Innovations (JECEI), vol. 8, no. 1, pp. 53–70, 2020.

[28] M. H. Moradi, F. Amiri, "Virtual inertia control in islanded microgrid by using robust model predictive control (RMPC) with considering the time delay," Soft Computing, vol. 25, pp. 6653–6663, 2021.

[29] R. Dhanalakshmi, S. Palaniswami, "Load frequency control of wind diesel hydro hybrid power system using conventional PI controller," European Journal of Scientific Research, vol. xx, pp. 630–641, 2011.

[30] D. I. Makrygiorgou, A. T. Alexandridis, "Nonlinear modeling, control and stability analysis of a hybrid ac/dc distributed generation system," in 2017 25th Mediterranean Conference on Control and Automation (MED), pp. 768–773, 2017.

[31] B. Kumar, S. Bhongade, "Load disturbance rejection based PID controller for frequency regulation of a microgrid," in 2016 Biennial International Conference on Power and Energy Systems: Towards Sustainable Energy (PESTSE), pp. 1–6, 2016.

[32] G. Mallesham, S. Mishra, A. N. Jha, "Ziegler-Nichols based controller parameters tuning for load frequency control in a microgrid," in 2011 International Conference on Energy, Automation and Signal, pp. 1–8, 2011.

[33] D. C. Das, A. K. Roy, N. Sinha, "GA based frequency controller for solar thermal–diesel–wind hybrid energy generation/energy storage system," International Journal of Electrical Power & Energy Systems, vol. 43, no. 1, pp. 262–279, 2012.

[34] D. C. Das, A. K. Roy, N. Sinha, "PSO based frequency controller for wind-solar-diesel hybrid energy generation/energy storage system," in 2011 International Conference on Energy, Automation and Signal, pp. 1–6, 2011.

[35] R. H. Kumar, S. Ushakumari, "Biogeography based tuning of PID controllers for Load Frequency Control in microgrid," in 2014 International Conference on Circuits, Power and Computing Technologies [ICCPCT-2014], pp. 797–802, 2014.

[36] A. Kumar, G. Shankar, "Quasi-oppositional harmony search algorithm based optimal dynamic load frequency control of a hybrid tidal–diesel power generation system," IET Generation, Transmission & Distribution, vol. 12, no. 5, pp. 1099–1108, 2018.

[37] N. Divya, S. Manoharan, J. Arulvadivu, P. Palpandian, "An efficient tuning of fractional order PID controller for an industrial control process," Materials Today: Proceedings, vol. 57, pp. 1654–1659, 2022.

[38] S. Khosravi, M. T. Hamidi Beheshti, H. Rastegar, "Robust control of islanded microgrid frequency using fractional-order PID," Iranian Journal of Science and Technology, Transactions of Electrical Engineering, vol. 44, pp. 1207–1220, 2020.

[39] V. Skiparev, K. Nosrati, A. Tepljakov, E. Petlenkov, Y. Levron, J. Belikov, J. M. Guerrero, "Virtual Inertia Control of Isolated Microgrids Using an NN-Based VFOPID Controller," IEEE Transactions on Sustainable Energy, vol. xx, pp. xx–xx, 2023.

[40] F. Babaei, Z. B. Lashkari, A. Safari, M. Farrokhifar, J. Salehi, "Salp swarm algorithm- based fractional- order PID controller for LFC systems in the presence of delayed EV aggregators," IET Electrical Systems in Transportation, vol. 10, no. 3, pp. 259–267, 2020.

[41] F. Babaei, A. Safari, "SCA based fractional-order PID controller considering delayed EV aggregators," Journal of Operation and Automation in Power Engineering, vol. 8, no. 1, pp. 75–85, 2020.

[42] S. Asgari, A. A. Suratgar, M. Kazemi, "Feedforward fractional order PID load frequency control of microgrid using harmony search algorithm," Iranian Journal of Science and Technology, Transactions of Electrical Engineering, vol. 45, no. 4, pp. 1369–1381, 2021.

[43] E. Çelik, "Design of new fractional order PI–fractional order PD cascade controller through dragonfly search algorithm for advanced load frequency control of power systems," Soft Computing, vol. 25, no. 2, pp. 1193–1217, 2021.

[44] M. Bhuyan, D. C. Das, A. K. Barik, S. C. Sahoo, "Performance assessment of novel solar thermal-based dual hybrid microgrid system using CBOA optimized cascaded PI-TID controller," IETE Journal of Research, vol. xx, pp. 1–18, 2022.

[45] M. Ali, H. Kotb, K. M. Aboras, N. H. Abbasy, "Design of cascaded pi-fractional order PID controller for improving the frequency response of hybrid microgrid system using gorilla troops optimizer," IEEE Access, vol. 9, pp. 150715–150732, 2021.

[46] A. R. Moazzeni, E. Khamehchi, "Rain optimization algorithm (ROA): A new metaheuristic method for drilling optimization solutions," *Journal of Petroleum Science and Engineering, vol. 195, pp. 107512, 2020.

[47] I. V. Pustokhina, D. A. Pustokhin, P. T. Nguyen, M. Elhoseny, K. Shankar, "Multi-objective rain optimization algorithm with WELM model for customer churn prediction in telecommunication sector," Complex & Intelligent Systems, pp. 1–13, 2021.

[48] S. Kumar, R. P. Mahapatra, "Design of multi-warehouse inventory model for an optimal replenishment policy using a rain optimization algorithm," Knowledge-Based Systems, vol. 231, pp. 107406, 2021.

All Authors

Farhad Amiri was born in Ilam. He received his MSc and PhD degrees in electrical engineering in 2017 and 2022, respectively, from Bu-Ali Sina University. He also received his post-doctoral (Electrical engineering) in 2024 from the National Elites Foundation of Iran. His research interests include dynamic and transient performance of power system, control, Microgrid and renewable energy.

Mohammad Hassan Moradi was born in Nowshahr, Mazandaran, Iran. He obtained his B.Sc., M.Sc. and PhD from Sharif University of Technology, Tarbiat Modares University and Strathclyde University in Glasgow, Scotland in 1991, 1993 and 2002 respectively. His research interests include New and Green Energy, Microgrid Modeling and Control, DG Location and Sizing in Power System, photovoltaic systems and power electronics, Combined Heat and Power Plant, Power Quality, Supervisory Control, Fuzzy Control.